# Growth, microstructure, and field-emission properties of synthesized diamond film on adamantane-coated silicon substrate by microwave plasma chemical vapor deposition

Rajanish N. Tiwari and Li Chang

Citation: Journal of Applied Physics **107**, 103305 (2010); doi: 10.1063/1.3427436
View online: http://dx.doi.org/10.1063/1.3427436
View Table of Contents: http://scitation.aip.org/content/aip/journal/jap/107/10?ver=pdfcov
Published by the AIP Publishing

# Growth, microstructure, and field-emission properties of synthesized diamond film on adamantane-coated silicon substrate by microwave plasma chemical vapor deposition

Rajanish N. Tiwari[a] and Li Chang[a]
*Department of Materials Science and Engineering, National Chiao Tung University, Hsinchu, Taiwan 300, Republic of China*

(Received 20 November 2009; accepted 3 April 2010; published online 24 May 2010)

Diamond nucleation on unscratched Si surface is great importance for its growth, and detailed understanding of this process is therefore desired for many applications. The pretreatment of the substrate surface may influence the initial growth period. In this study, diamond films have been synthesized on adamantane-coated crystalline silicon {100} substrate by microwave plasma chemical vapor deposition from a gaseous mixture of methane and hydrogen gases without the application of a bias voltage to the substrates. Prior to adamantane coating, the Si substrates were not pretreated such as abraded/scratched. The substrate temperature was ~530 °C during diamond deposition. The deposited films are characterized by scanning electron microscopy, Raman spectrometry, x-ray diffraction, and x-ray photoelectron spectroscopy. These measurements provide definitive evidence for high-crystalline quality diamond film, which is synthesized on a SiC rather than clean Si substrate. Characterization through atomic force microscope allows establishing fine quality criteria of the film according to the grain size of nanodiamond along with SiC. The diamond films exhibit a low-threshold (55 $V/\mu m$) and high current-density (1.6 $mA/cm^2$) field-emission (FE) display. The possible mechanism of formation of diamond films and their FE properties have been demonstrated. © *2010 American Institute of Physics*. [doi:10.1063/1.3427436]

## I. INTRODUCTION

The synthesis of diamond film by chemical vapor deposition (CVD) has been widely demonstrated in the past few decades, due to the combination of its outstanding physical and chemical properties, such as wide band gap, negative electron affinity, chemical inertness, high carrier mobility, excellent biological compatibility, good optical transparency, excellent thermal conductivity, high propagation speed of acoustic wave, and the greatest hardness. The unique properties of diamond make it an ideal material for a wide range of scientific and technological applications such as optics, microelectronics, tribological, thermal management, biomedical, DNA sensor, and so on.[1–6]

Recently, diamond deposition on the nondiamond substrates is performed by nucleation processing step. Nucleation, corresponds to the formation of diamond nuclei, i.e., the smallest thermodynamically stable island, at the substrate surface. Nucleation procedures have been developed by performing either *ex situ* treatments on the substrate such as scratching with powders (diamond, carbide, oxides, silicides, nitride carbides, borides, and etc.) or *in situ* methods before CVD growth such as dc or ac voltage bias technique.[7–9] The former process leads to inhomogeneous density of the nuclei as well as deleterious surface, while the later one is limited by the conductivity of the substrate. The deleterious surface and roughening resulting from scratching is not friendly with numerous applications such as optical windows, masks used in photolithography, and so on, while nonscratching method for growing thick diamond film with high nucleation density are particular significance. Currently several groups have used different seeding materials (without scratching) such as graphite fibers, fullerenes clusters, hydrocarbon oil, and thin films of different types of carbon for the diamond deposition.[10–12] However, despite rapid progress, the growth of diamond film on the silicon substrate by microwave plasma CVD (MPCVD) still require nucleation step for improvement in terms of yield, quality, purity, and uniformity to synthesis of diamond at relatively low temperature and pressure.

Here we introduce the application of adamantane for diamond synthesis. Adamantane ($C_{10}H_{16}$) is one of a series of carbon structure, very stable crystalline compound, and highly symmetric molecule with point group symmetry, Td. Adamantane is the smallest possible diamondoids (chemical formula $C_{(4n+6)}H_{(4n+12)}$, where $n=0,1,2,3,\ldots$), consisting of 10 carbon atoms arranged as a single diamond cage surrounded by 16 hydrogen atoms, as shown in Scheme 1. A cagelike structure is formed with six $CH_2$ and four CH groups giving rise to a molecular structure with four cyclohexane rings in chair form. Its structure has zero strain as all C–C–C bond angles are 109.45° with a corresponding bond length of 1.54 Å and C–H bond length is 1.1 Å. The density of adamantane is 1.07 $g/cm^3$. Adamantane does not melt at ambient pressure but sublimates. Partial breakdown of adamantane is known to yield carbon clusters ($C_nH_x$), where $n=3$, 5, 6, 7, 8, and 9, of significant abundance.[13] Matsumoto and Matsui[14] in their study of diamond synthesis by CVD two decades ago suggested that hydrocarbon cage molecules

[a]Authors to whom correspondence should be addressed. Electronic addresses: rajanisht@gmail.com and lichang@cc.nctu.edu.tw. Tel.: 886-3-5155373. FAX: 886-3-5724727.

 

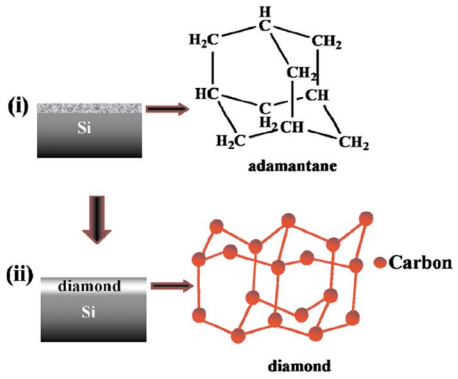


SCHEME 1. Schematic diagram showing diamond synthesis in two steps; (i) adamantane deposited on silicon surface by hotplate method, and (ii) diamond growth by MPCVD.

such as adamantane are possible embryos for the homogeneous nucleation of diamond, there are rarely studies of diamond synthesis related with diamondoids. Previously, Leroy *et al.* and Giraud *et al.* had been used 2, 2-divinyladamantane molecules (adamantane derivative) for diamond nucleation and growth on the silicon (111) substrate at 850 °C.[7,10] Another important issue in particular CVD diamond, since early 1980 report is the high deposition temperature (700–900 °C), which limits only on thermal stable substrates. The deposition of high quality diamond at low temperature is still challenging even if some studies reported diamond deposition at temperature below 550 °C.[15–18]

Here we report a simple method for the synthesis of good-quality diamond film on adamantane ($C_{10}H_{16}$)-coated Si surface by the MPCVD at relatively low temperature. The rate of film growth in 0.6% methane ($CH_4$) in hydrogen ($H_2$) was 0.5 $\mu$m $h^{-1}$. A quantitative estimation of minimum temperature for diamond deposition is proposed. Interest, which exists in the development of CVD diamond processes at low temperature, is to deposit high quality diamond film at high growth rate. The advantages for using the adamantane are that it is not much expensive and easily commercially available. The deposited diamond crystallites films are well faceted. Their excellent field-emission (FE) property is also reported.

## II. EXPERIMENTAL

The schematic diagram of diamond synthesis on the adamantane-coated Si substrate is shown in Scheme 1. The commercial adamantane powders in 99+% purity were obtained from Sigma-Aldrich Chemie GmbH (CAS:281–23–2). The deposition processes of the diamond films are described as follows: mirror-polished p -type (100) silicon wafers with dimensions of $1 \times 1$ $cm^2$ without any mechanical pretreatment were used as the substrates. The substrates were ultrasonically cleaned with acetone and alcohol for 10 min, respectively, and then dried with nitrogen. The cleaned samples were dipped into buffer-oxide-etch solution (10% HF) for 5 min to remove the native oxide layer from the Si surface. Further, the cleaned Si samples were fixed onto a ceramic plate. The adamantane powder was kept in a ceramic crucible and covered with fixed Si substrates onto ceramic plate, and then placed on a hot plate at 250 °C (hereafter called hotplate method) for 5 min, which allowed to deposit a thick adamantane films (thickness ~0.9 mm) onto the Si surface. The thickness of deposited adamantane on Si was manually measured by scale. The distance between the fixed Si substrates and adamantane powder was ~2 cm. The adamantane-coated Si substrates were then placed on a Mo-disk holder for diamond growth in an AsTeX-type MPCVD system. The detailed processing parameters for MPCVD are as follows: the total pressure was 20 torr, the microwave power was 350 W, the total flow rate was 200 SCCM (where "SCCM" denotes cubic centimeter per minute at STP), deposition time was varied from 15 to 270 min, and the temperature was ~530 °C as measured by an optical pyrometer. Finally, the samples were allowed to cool down to ambient temperature in the presence of hydrogen gas at 10 torr to etch the nondiamond phases that remained after the diamond growth.

The surface morphology was examined in a field-emission scanning electron microscope (SEM, JEOL JSM-6700F). Chemical compositions of the surface were characterized by x-ray photoelectron spectroscopy (XPS, Thermo VG 350 F, Mg $K\alpha$ x-ray source). The crystallinity of diamond was evaluated with an x-ray diffractometer (XRD) (Siemens XRD D5000). Raman spectroscopy (LABRAM HR800) was performed in a system using an Ar laser (laser-beam wavelength: 514.5 nm), which could be focused to ~1 $\mu$m diameter for micromode operation. The surface morphology of plane regions of Si substrate was evaluated using atomic force microscopy (AFM, Digital Instruments Nanoscope, D-3100) at a scan size of 5 $\mu$m and a scan rate of 1 Hz.

The FE measurements were carried out in a vacuum chamber with a base pressure of $10^{-6}$ torr at room temperature by using a parallel cathode-anode setup[19] with a 1 mm diameter molybdenum tip as anode. The distance between the anode tip and the cathode was controlled at 12 $\mu$m by a digital micrometer controller and an optical microscope. The current-voltage characteristics of the films were acquired using a Keithley 237 electron source unit and were modeled with the Fowler–Nordheim (F–N) theory.[20]

## III. RESULTS AND DISCUSSION

After coating of adamantane on Si substrate at 250 °C, an optical microscope was used to characterize the surface morphology of the adamantane layer. Figure 1(a) shows the continuous adamantane film has been coated on the Si (100) surface. The inset high-magnification optical image in Fig. 1(a) shows the grain size of adamantane in several micrometers. We believe that the micrometer sized adamantane consisted of several ultrasize or nanosize adamantane particles. These ultrasize or nanosize adamantane particles bonded together with weak van der Waal forces. The coated adamantane on Si substrate was then analyzed by XRD. The XRD pattern in Fig. 1(a) presents sharp and well-defined peaks, and the observed diffraction peaks at $2\theta = 16.3°$, 18.8°, 26.7°, 31.5°, 32.9°, 41.7°, 47.1°, 50.3°, 54.9°, 57.7°, 59.1°, 71.3°, and 72.0° correspond to the interplanar spacings of adaman-

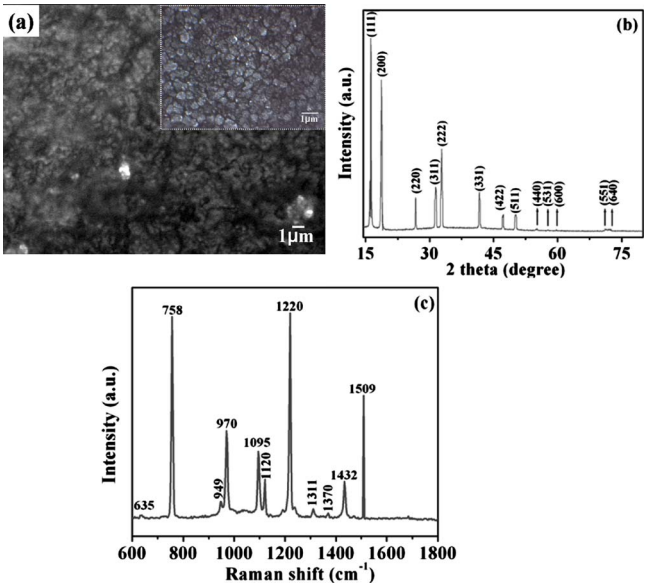


FIG. 1. (Color online) (a) Optical image, inset: high-magnification image of the adamantane, (b) XRD pattern of adamantane, and (c) Raman spectrum of the adamantane coating layer on Si (100) substrate.

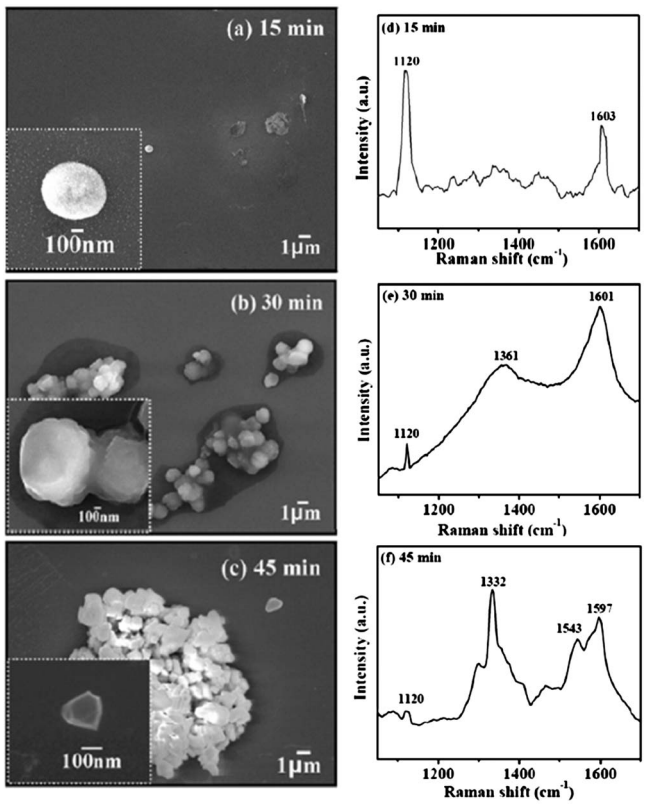


FIG. 2. Plan-view SEM images and micro-Raman spectra after growth for deposition times of (a) and (c) 15 min, (b) and (d) 30 min, and (c) and (f) 45 min.

tane {111}, {200}, {220}, {311}, {222}, {331}, {422}, {511}, {440}, {531}, {600}, {551}, and {640}, respectively. The experimental $2\theta$ values are consistent with the standard Joint Committee for Powder Diffraction Standard (JCPDS) values (JCPDS file nos.: 22–1529 and 31–1505). Further, the adamantane-coated Si substrate was also evaluated using Raman spectroscopy (LABRAM HR800). Intense Raman peaks in the range of 600–1800 $cm^{-1}$ are shown in Fig. 1(c). We observed the multiple Raman peaks at 635, 758, 949, 970, 1095, 1120, 1220, 1312, 1370, 1432, and 1509 $cm^{-1}$. These peaks are due to different modes of hydrocarbon (C-H) in adamantane molecule. The Raman peaks at 635, 758, 949, and 970 were due to CCC bend/CC stretch modes while other Raman peaks at 1095, 1120 and 1220, 1312, and 1370 $cm^{-1}$ was due to doubly-degenerated CH wag/$CH_2$ twist modes. The Raman peaks at 1432 and 1509 $cm^{-1}$ may be due to E $CH_2$ scissor mode.[21]

Further, the adamantane-coated Si substrates were placed in a MPCVD reactor for diamond deposition. In the reactor, the plasma was formed by activating the mixture of gases (0.6% $CH_4$ in $H_2$). To know the diamond nucleation from adamantane molecules, we placed the adamantane-coated Si substrates in the MPCVD reactor at various deposition times (15 to 45 min), as shown in Fig. 2. The surface morphology of the synthesized particles on the Si substrate was examined with field-emission SEM and their characteristics are shown in Fig. 2. The SEM image in Fig. 2(a) shows that the tiny particles are formed in a short time (15 min). The inset high-magnification image in Fig. 2(a) shows that the tiny particles are surrounded by several hundred nanometer-sized particles. The micro-Raman spectrum from these particles in Fig. 2(d) shows the major peaks at 1120 and 1603 $cm^{-1}$ are observed, indicating that adamantane has been decomposed during 15 min deposition. The Raman peak at 1603 $cm^{-1}$ is the G band of $sp^2$ carbon bonding, while the Raman peak at 1120 $cm^{-1}$ is not well understood about the bonding characteristics but it is often observed in Raman spectra of nanocrystalline diamond films.[22–24] Previous studies have shown that the Raman peak at 1120 $cm^{-1}$ usually appears for nanocrystals 1–2 nm in diameter or carbon clusters of $sp^3$ bonded material. However, this peak can also appear at 1150 $cm^{-1}$ but only in very poorly organized graphite, being related to structures of a mixed $sp^2$–$sp^3$ nature.[25–27] It is widely believed that the peak at 1120 $cm^{-1}$ originated from the presence of confined phonon modes in diamond.[28,29] After having been decomposed, the surrounded nanosized particles were melted after 30 min deposition), and formed clusters of microsized carbon particles, as shown in Fig. 2(b). The high-magnification SEM image [inset in Fig. 2(b)] shows the particles have bright contrast while melted regions show dark contrast (these dark regions may be formed due to $sp^2$ phase transformation from adamantane molecules). The Raman spectrum from these particles is shown in Fig. 2(e). We observed Raman peaks at 1120 $cm^{-1}$, along with 1361 and 1601 $cm^{-1}$ show the D and G band, respectively. The Raman peak at 1120 $cm^{-1}$ corresponds to nanocrystals diamond (described above), while the D band (may be comes from dark region) peak is usually attributed to disorder carbon, showing the transformation from adamantane to $sp^2$, while the Raman peak at 1601 $cm^{-1}$ shows the graphitic particles. Furthermore, after 45 min deposition, we did not notice dark regions (melt) which was observed in Fig. 2(b) (30 min deposition). We observed only clusters of carbon particles along with few nanosized particles on the Si substrate. It seems that after 45 min deposition the dark re-

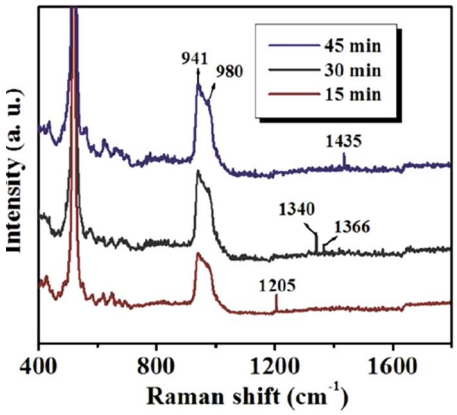


FIG. 3. (Color online) Raman spectra of adamantane-coated Si substrates after 15, 30, and 45 min deposition.

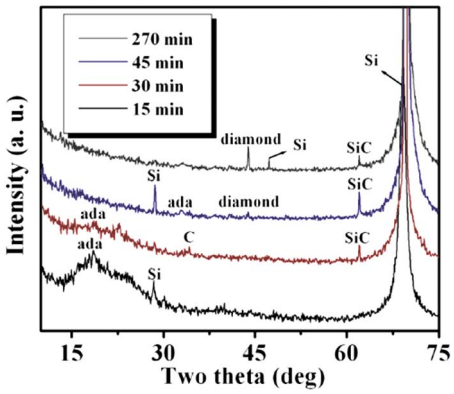


FIG. 4. (Color online) XRD patterns of adamantane-coated Si substrates after 15, 30, and 270 min deposition.

gions [in Fig. 2(b)] are fully transformed into carbon phase. The high-magnification SEM image of nanoparticles in Fig. 2(c) shows the crystalline diamond particles are also formed. The Raman spectrum from these particles is shown in Fig. 2(f). Figure 2(f) shows the multi Raman peaks at 1120, 1332, 1543, and 1596 $cm^{-1}$. The Raman peaks at 1120 $cm^{-1}$ and 1332 $cm^{-1}$ are supported to the diamond formation has occurred, while the Raman peaks at 1543 $cm^{-1}$ and 1596 $cm^{-1}$ correspond amorphous carbon (a-C:H) and graphite particles, respectively.

In addition, after 15, 30, and 45 min depositions the Raman spectra from the plane (not from particles) a region of Si surface is shown in Fig. 3. The Raman spectrum of adamantane shown in Fig. 1(c), strong peaks observed at 758 $cm^{-1}$ and 1220 $cm^{-1}$ which corresponds to the CC stretch and doubly-degenerate $CH_2$ twist mode, respectively. After short time (15 min) treatment in the MPCVD reactor, such peaks were not observed. Our perception is that in the CVD reactor, some adamantane molecules would have pumped out while a fraction of adamantane molecules would have decomposed either in the form of small molecules [$(C_nH_x)$, where n=3, 5, 6, 7, 8, and 9] or its clusters. Therefore, we noticed that the two strong peaks at approximately 941 and 978 $cm^{-1}$ from plane region (not from particles), after various times (15, 30, and 45 min) deposition. The Raman peaks at 941 and 978 $cm^{-1}$ corresponds to SiC.[30,31] We also observed weak Raman signals at 1205, 1344, 1366, and 1435 $cm^{-1}$ in the 15, 30, and 45 min deposition, as shown in Fig. 3. The Raman peak at 1205 $cm^{-1}$ corresponds to a mixed bond arising between $sp^2$ and $sp^3$ bonded carbon. After 30 min deposition, we observed peaks at 1344 and 1366 $cm^{-1}$ show the D band, while the Raman peak at 1435 $cm^{-1}$ corresponds to amorphous carbon peak after 45 min deposition. This shows that significant amount of non-diamond phase is also formed in the early stage depositions.

Further, the XRD pattern of these samples (after 15, 30, and 45 min depositions) is shown in Fig. 4. In short time (15 min) deposition, we noticed that the fraction of crystalline adamantane {200} particles is distributed on the Si surface. The average thickness of adamantane on the Si surface is ~90 nm, as shown in Fig. 5(a). While after longer time (30 min) deposition the adamantane started to transform into carbon phase. Therefore, we observed a diffraction peaks at $2\theta$=18.8° and 34.22° along with sharp 3C-SiC {220} peak at $2\theta$=61.7°.[32] The peak at 18.8° corresponds to adamantane {200}, while 34.22° shows the presence of carbon {123}. The experimental $2\theta$ values of carbon are consistent with the standard JCPDS values (JCPDS file no.: 50–0926). In addition Si peaks, we observed the diamond {111} along with 3C-SiC {220} after 45 min deposition. Thus, we believe that diamond nucleation has been started after 45 min deposition. We also observed that the very weak signal of adamantane {222} at 32.9° indicates that the minor fraction of adamantane is still left on the Si surface. As the XRD $2\theta$ peak at 43.9° is characteristic of crystalline diamond, it suggests that the diamond phase has indeed been deposited after 45 min

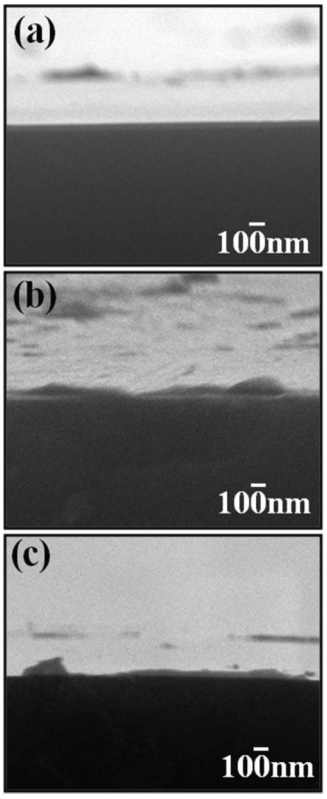


FIG. 5. Cross-sectional SEM images of adamantane-coated Si substrates treated with various times: (a) 15 min, (b) 30 min, and (c) 45 min.

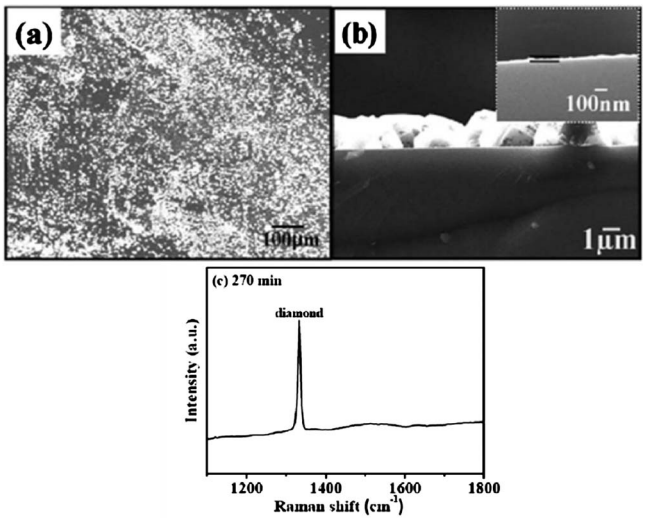


FIG. 6. SEM images of deposited diamond in (a) plan–view and (b) cross-section view, inset: high-magnification image of interlayer, (c) Raman spectrum after synthesized diamond (growth time 270 min) on Si surface pretreated with adamantane.

deposition. This is the consistent our SEM and Raman data. It is also clear that the first SiC formed and then diamond deposited over it. We noticed that the average thickness of either carbon species or 3C-SiC after 30 min and 45 min depositions are ~110 nm, and 130 nm, respectively, indicating that thickness of carbon contents along with SiC increases with increasing the deposition times, as shown in Fig. 5.

Further, the surface morphology of the synthesized diamond films on the Si substrate were examined with SEM and their characteristics are shown in Fig. 6. It is clear that the fraction of deposited adamantane molecules have converted into the carbon species (Fig. 2) in the CVD plasma and it may assist diamond nucleation. Figure 6 shows plan-view and cross-section SEM images of synthesized diamond on adamantane-coated Si substrate after 270 min deposition. In our previous studies, we have shown that that the average size and thickness of well-faceted diamond are ~1.6 $\mu$m and ~2 $\mu$m, respectively, as shown in Figs. 6(a) and 6(b).[33] We also noticed that the either adamantane or carbon species reacted with Si surface and formed SiC interlayer between the diamond and Si substrate. The inset high-magnification SEM image in Fig. 6(b) shows that the ~50 nm SiC layer has been formed during diamond growth. Previous studies have shown that silicon carbide (SiC) forms readily after diamond growth starts.[34–36] The SiC interlayer also influence the quality of diamond. The growth rate of diamond is estimated to be ~0.5 $\mu$m/h, and the density of diamond is $\sim 10^8$ cm$^{-2}$ on the adamantane-coated substrate. In our previous studies, we have shown that the adamantane precursor not only increases the quality, crystallinity, and growth rate but also enhances the yield than that of without adamantane-coated.[37] Further, The XRD pattern also support formation of the microdiamond crystalline film, as shown in Fig. 4. In addition to Si peaks, the XRD pattern in Fig. 4 presents sharp and well-defined peaks, and the observed diffraction peaks at $2\theta$=43.9° and 61.7° correspond to the interplanar spacings of diamond {111} and crystalline 3C-SiC {220} respectively. In addition, the micro-Raman spectrum of the diamond film is shown in Fig. 6(c). The characteristic feature of diamond at 1332 cm$^{-1}$ is clearly observed, the full width at half-maximum of the peak is determined to be 5.8 cm$^{-1}$. The sharp Raman peak suggests the high quality microdiamonds have been synthesized on the Si surface. The XRD and Raman results show that the high-crystalline quality diamond film has been synthesized at 530 °C.

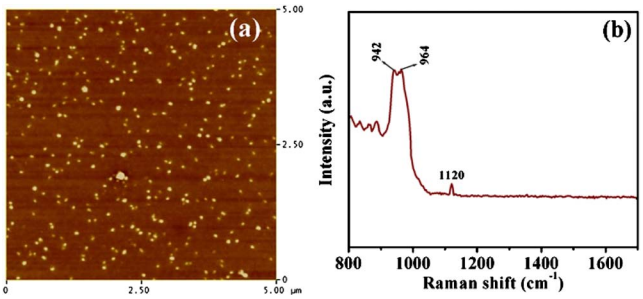


FIG. 7. (Color online) (a) AFM and (b) corresponding Raman spectrum of plane region where we did not observe microdiamond film after 270 min diamond growth.

Moreover, the microdiamond films were not uniformly distributed on the Si surface. To know the surface effect (plane regions of Si surface where we did not observe the microdiamond film) after diamond deposition (270 min), the plane regions of Si surface were characterized by AFM and Raman spectroscopy, as shown in Fig. 7. Here, we used tapping-mode AFM on a length scale of $5\times5$ $\mu$m$^2$ to determine the surface roughness as well as affect the Si surface after diamond deposition. Figure 7(a) shows the crystalline tiny particles have also been formed on the Si surface (after diamond deposition). We have used Raman spectroscopy to characterize these nanoparticles, as shown in Fig. 7(b). We observed that the two sharp Raman signals at 941 and 964 cm$^{-1}$ and weak signal at 1120 cm$^{-1}$. These sharp two peaks at 941 and 964 cm$^{-1}$ are come from SiC particles[38] while nanodiamond peak at 1120 cm$^{-1}$ (described above). It seems that the nanodiamond particles have also been formed in the plane regions along with SiC.

In addition, we have used XPS to characterize the surface chemical composition of the adamantane-coated Si surface after diamond growth. The XPS survey spectrum is shown in Fig. 8, which allows measure of the carbon 1*s* core-level signal considered as an indicator for the quantity of carbon attached to the Si surface treatment. Apart from the expected peaks from elements of the diamond surface (C), surface contamination along with oxygen containing molecules have been detected. An XPS survey shows strong signals of carbon C 1*s* at 285.2 eV, attributed to the C-C bond in diamond films. In fact, inset XPS high-resolution spectrum of carbon in Fig. 8 showed the C 1*s* signal revealed two peaks: the first peaks at 285.2 eV is the characteristics of C-C bonding and other peak at 283.7 eV is the characteristics of C–Si bonding. The part of the oxygen signal at 532.7 eV attributed to the O–Si bond in $SiO_2$.[39,40] The weak signals of silicon Si 2*p* and Si 2*s* at 99 and 151 eV, indicates that the most of silicon surface is covered by diamond films.[41] On the

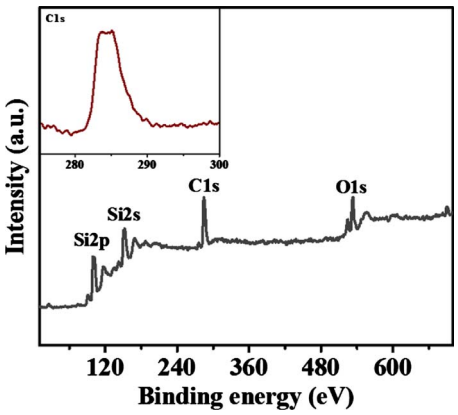


FIG. 8. (Color online) The XPS survey spectrum of diamond/Si, inset: high-resolution spectrum of the C 1*s* region.

basis of XPS results, we confirm the existence of diamond as well as SiC. This is the consistent of our SEM, XRD, and Raman results.

After diamond growth, the FE properties were investigated. Figure 9 shows the relation of emission current density as a function of applied electrical field of continous well-faceted diamond film. The FE characteristics of sample has been carried out by defining a threshold field $\xi$th corresponding to current density of 10 $\mu A/cm^2$. The inset in Fig. 9 is the corresponding F–N plot, $\ln(J/E^2)$ versus 1/E, of the corresponding FE data, indicating that the field electron emission of well-faceted continuous diamond film follows the classic FE mechanism. The turn-on field of diamond film at the current density of 0.0011 $mA/cm^2$ is approximately 55 $V/\mu m$. The threshold field at an emission current density of 1 $mA/cm^2$ is about 92 $V/\mu m$. The threshold field at which an emission current density of 1.6 $mA/cm^2$ is achieved, being considered as a figure of merit for conventional flat panel displays. This value is better than previously reported values for various field-emitting materials including microdiamond films, but worse than that of oriented nanodiamond, submicrodiamond, and microdiamond film.[5,42,43] The SEM image in Fig. 6(a) and 6(b) shows the well-faceted microdiamond films (thickness: ~2 $\mu m$) have been deposited on the Si surface. Probably, the diamond edges can be acted as electron emitters, resulted high current density 1.6 $mA/cm^2$ for an applied field of 96 $V/\mu m$. The low

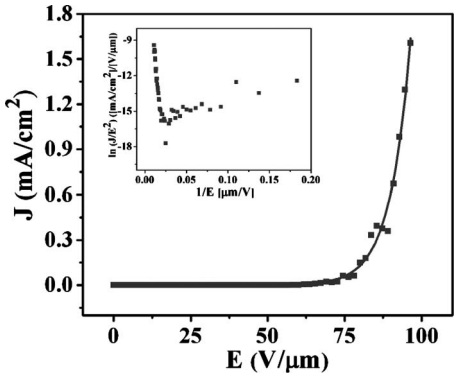


FIG. 9. Emission current density as a function of applied electrical field for diamond plates and inset corresponding F–N plot.

turn-on field and high current density of diamond film on the Si surface could be assigned following factors: first, the well-faceted edges [Figs. 6(a) and 6(b)] may enhance the FE properties.[5] Another reason may be well-faceted diamond films act like separated emitting edge, which not only could have a large field enhancement factor, but could also effectively depress the screen effect.

In this study, the microsized diamond films have been synthesized on adamantane-coated Si substrate by MPCVD at relatively lot temperature. The synthesized diamond on adamantane-coated Si substrate may provide some essential information to understand growth mechanisms.

In microwave plasma, the mixture of gases (methane/hydrogen) can produce hydrogen and. methyl radicals ($CH_3^*$) as shown in the following reaction

$$CH_4 + H^* = CH_3^* + H_2.$$

When the adamantane-coated Si substrate placed in the CVD reactor, the adamantane sublimated in short time deposition and mixed in gaseous plasma. Probably, fraction of adamantane molecules are distributed on the Si surface, while most of adamantane molecules have pumped out from the MPCVD reactor. During the longer treating time (after 30 and 45 min deposition), dissociated carbon/hydrocarbon radicals impinge and absorbed in the molten adamantane molecules (melting point 270 °C). When the carbon-containing adamantane molecules tends to saturate, phase separation, and carbon precipitating occur to form tiny clusters may exist in liquid phase. Then, when critical radii arrive, liquid carbon nuclei will solidify. So, tiny clusters may exist in liquid phase and coarsening easily to form the nucleuses of diamond. In previous study, we have shown that the hydrogen abstraction is one of the highly possible mechanisms for diamond nucleation in the gas phase (sublimated and mixed in the gaseous plasma and then deposited on the Si surface).[33,37] In the intermediate growth steps, as shown in Figs. 2 and 3 indicates that the adamantane converts into graphite phase intermixed with amorphous carbon, enhance the diamond growth. A similar observation (graphite transform into diamond) of diamond deposition on the Si substrate have been reported previously.[44,45] In previous studies, Kompoulos *et al.* and Feng *et al.* have observed the diamond films on thin amorphous carbon coated Si substrates, while Barnes *et al.* had noticed that the high density of diamond nucleation on the Si substrate which was first scratched with diamond paste and then deposited with a nondiamond amorphous carbon film. In our case, the quality and crystallinity of deposited diamond films on the adamantane-coated Si substrates is better than previously reported.[9,11,46]

And finally, methane gas species favor to individual nuclei grows three dimensionally by a vapor-solid growth. The hydrogen atom (H-atom) abstraction from the $CH_4$ molecules (shown in reaction) will form methyl radicals ($CH_3^-$) or other active hydrocarbons. The growth of microcrystalline diamond film proceed through surface chemical reactions such as the formation and migration of hydrocarbon in the vicinity of surface, hydrogen abstraction, dehydrogenation of absorbed complexes, recombination of hydrogen atoms, and so on., which can be more than 99% $sp^3$ bonded carbon, and

do possess many of the properties of natural diamond. Often some degree of nondiamond carbon is incorporated during this nucleation. The atomic hydrogen or ions prevents the formation of nondiamond carbon impurity on the surface or etch the graphitic state and favor to diamond growth. From the SEM views, it is clear that the after forming the stable crystalline particles, the low concentrations methane species were grown in preferred (111) facets of diamond, as shown in Fig. 4. The exact mechanism for such diamond nucleation from adamantane molecules might be clarified with further experimental evidence from detailed examination of film morphology and microstructure at atomic resolution.

## IV. CONCLUSIONS

In summary, we present a facile and unique approach for the synthesis of good-quality diamond film on adamantane-coated Si substrate by microwave plasma CVD. The characterization of synthesized products revealed that the adamantane first convert into either graphite or carbon and then grown into diamond films. SEM shows the well-faceted diamond films (thickness in $\sim 2$ $\mu$m) with $\sim 50$ nm SiC interlayer has been formed. While XRD and Raman spectrum show the good crystallinity and high quality of diamond film. XRD and XPS show diamond film deposited on the SiC rather than clean Si substrate. AFM shows the nanodiamond particles also formed along with microdiamond film. The deposited diamond films exhibit good FE characteristics of reasonably low-threshold voltage and high current density.

## ACKNOWLEDGMENTS

The authors would like to thank the National Science Council of the Republic of China, Taiwan, for financially supporting this research under Contract Nos. NSC96-2622-E-009-002-CC3 and 98-2221-E-009-042-MY3.

[1] S. D. Wolter, M. T. McClure, J. T. Glass, and B. R. Stoner, Appl. Phys. Lett. **66**, 2810 (1995).
[2] J. K. Yan and L. Chang, Nanotechnology **17**, 5544 (2006).
[3] A. A. Fokin, B. A. Tkachenko, N. A. Fokina, H. Hausmann, M. Serafin, J. E. P. Dahl, R. M. K. Carlson, and P. R. Schreiner, Chem.-Eur. J. **15**, 3851 (2009).
[4] A. Krueger, Chem.-Eur. J. **14**, 1382 (2008).
[5] H. G. Chen and L. Chang, Diamond Relat. Mater. **18**, 141 (2009).
[6] N. Yang, H. Uetsuka, E. Osawa, and C. E. Nebel, Angew. Chem., Int. Ed. **47**, 5183 (2008).
[7] E. Leroy, O. M. Kuttel, L. Schlapbach, L. Giraud, and T. Jenny, Appl. Phys. Lett. **73**, 1050 (1998).
[8] R. J. Meilunas, R. P. H. Chang, S. Liu, and M. M. Kappes, Appl. Phys. Lett. **59**, 3461 (1991).
[9] P. N. Barnes and R. L. C. Wu, Appl. Phys. Lett. **62**, 37 (1993).
[10] A. Giraud, T. Jenny, E. Leroy O. M. Küttel, L. Schlapbach, P. Vanelle, and L. Giraud, J. Am. Chem. Soc. **123**, 2271 (2001).
[11] Z. Feng, K. Komvopoulos, D. B. Bogy, J. W. Ager, S. Anders, A. Anders, Z. Wang, and I. G. Brown, J. Appl. Phys. **79**, 485 (1996).
[12] A. A. Morrish and P. E. Pehrsson, Appl. Phys. Lett. **59**, 417 (1991).
[13] M. Umeno, M. Noda, H. Uchida, and H. Takeuchi, Diamond Relat. Mater. **17**, 684 (2008).
[14] S. Matsumoto and Y. Matsui, J. Mater. Sci. **18**, 1785 (1983).
[15] L. Wang, Y. Wang, J. Zhou, and S. Ouyang, Mater. Sci. Eng., A **475**, 17 (2008).
[16] L. Dong, B. Ma, and G. Dong, Diamond Relat. Mater. **11**, 1697 (2002).
[17] I. Schmidt and C. Benndorf, Diamond Relat. Mater. **10**, 347 (2001).
[18] Y. Liou, A. Inspektor, R. Weimer, D. Knight, and R. Messier, J. Mater. Res. **5**, 2305 (1990).
[19] C. Y. Lee, J. S. Lin, N. I. Lin, and H. F. Cheng, J. Appl. Phys. **97**, 054310 (2005).
[20] H. R. Fowler and L. Nordheim, Proc. R. Soc. London, Ser. A **119**, 173 (1928).
[21] J. Filik, J. N. Harvey, N. L. Allan, P. W. May, J. E. P. Dahl, S. Liu, and R. M. K. Carlson, Spectrochim. Acta, Part A **64**, 681 (2006).
[22] T. Sharda, T. Soga, T. Jimbo, and M. Uembo, Diamond Relat. Mater. **10**, 1592 (2001).
[23] T. Lin, Y. Yu, A. T. S. Wee, Z. X. Shen, and K. P. Loh, Appl. Phys. Lett. **77**, 2692 (2000).
[24] L. Fayette, B. Marcus, M. Mermoux, G. Tourillon, K. Laffon, P. Parent, and F. LeNormand, Phys. Rev. B **57**, 14123 (1998).
[25] S. Prawer, K. W. Nugent, and D. N. Jamieson, Diamond Relat. Mater. **7**, 106 (1998).
[26] V. Paillard, P. Melinon, V. Dupuis, A. Perez, J. P. Perez, G. Guiraud, and J. Formazero, Phys. Rev. **49**, 11433 (1994).
[27] W. S. Bacsa, J. S. Lannin, D. L. Pappas, and J. J. Cuomo, Phys. Rev. B **47**, 10931 (1993).
[28] J. Birrell, J. E. Gerbi, O. Auciello, J. M. Gibson, J. Johnson, and J. A. Carlisle, Diamond Relat. Mater. **14**, 86 (2005).
[29] A. T. Sowers, B. L. Ward, S. L. English, and R. J. Nemanich, J. Appl. Phys. **86**, 3973 (1999).
[30] M. Bechelany, A. Brioude, D. Cornu, G. Ferro, and P. Miele, Adv. Funct. Mater. **17**, 939 (2007).
[31] J. Wasyluk, T. S. Perova, S. A. Kukushkin, A. V. Osipov, N. A. Feoktistov, and S. A. Grudinkin, Mater. Sci. Forum **645**, 359 (2010).
[32] S. Intarasiri, A. Hallen, J. Lu, J. Jensen, L. D. Yu, K. Bertilsson, M. Wolborski, S. Singkarat, and G. Possnert, Appl. Surf. Sci. **253**, 4836 (2007).
[33] R. N. Tiwari and L. Chang, Appl. Phys. Express **3**, 045501 (2010).
[34] E. J. Corat, N. G. Ferreira, V. J. T. Alroldi, N. F. Leite, R. C. M. Barros, and K. Iha, J. Mater. Sci. Lett. **16**, 197 (1997).
[35] P. O. Joffreau, R. Haubner, and B. Lux, Int. J. Refract. Hard Met. **7**, 186 (1988).
[36] H. Kawarada, T. Suesada, and H. Nagasawa, Appl. Phys. Lett. **66**, 583 (1995).
[37] R. N. Tiwari, J. N. Tiwari, and L. Chang, Chem. Eng. J. **158**, 641 (2010).
[38] S. Nakashima and H. Harima, Phys. Status Solidi A **162**, 39 (1997).
[39] E. Maillard-Schaller, O. M. Kuettel, and L. Schlapbach, Phys. Status Solidi A **153**, 415 (1996).
[40] S. Gsell, S. Berner, T. Brugger, M. Schreck, R. Brescia, M. Fischer, T. Greber, J. Osterwalder, and B. Stritzker, Diamond Relat. Mater. **17**, 1029 (2008).
[41] R. Boukherroub, D. D. M. Wayner, G. I. Sproule, D. J. Lockwood, and L. T. Canham, Nano Lett. **1**, 713 (2001).
[42] P. T. Joseph, N. H. Tai, C. H. Chen, H. Niu, H. F. Cheng, W. F. Pong, and I. N. Lin, J. Phys. D: Appl. Phys. **42**, 105403 (2009).
[43] S. Arora and V. D. Vankar, Thin Solid Films **515**, 1963 (2006).
[44] Y. X. Han, H. Ling, J. Sun, M. Zhao, T. Gebre, and Y. F. Lu, Appl. Surf. Sci. **254**, 2054 (2008).
[45] W. R. L. Lambrecht, C. H. Lee, B. Segall, J. C. Angus, Z. Li, and M. Sunkara, Nature (London) **364**, 607 (1993).
[46] K. Komvopoulos and T. Xu, Diamond Relat. Mater. **9**, 274 (2000).